Assessing the Impact of the COVID-19 Recession on the S&P 500 Using Synthetic Control and Stochastic Volatility Modeling

Reetom Gangopadhyay, Youran Geng, Sayed AlGharbi

April 25, 2025

Abstract

This paper evaluates the causal effect of the COVID-19 recession on the S&P 500 index by combining the Synthetic Control Method (SCM) with stochastic volatility modeling via a custom Gibbs sampler. We define February 13, 2020, as the treatment onset and construct counterfactual return paths using both equity indices and an expanded donor pool including commodities. The mixed donor model reduces post-treatment tracking error and offers a more robust counterfactual. We then estimate stochastic volatility models separately on actual and synthetic return series to assess differences in market uncertainty. Posterior volatility trajectories are strikingly similar in the full sample but diverge modestly during the early COVID-19 window, suggesting a brief period of heightened uncertainty in actual returns. Our results highlight the strengths of using dual modeling frameworks to capture both return-level and risk-based treatment effects during macroeconomic shocks.

1 Introduction

The COVID-19 pandemic triggered a historic global recession, with substantial disruptions to financial markets. The S&P 500—one of the most widely tracked equity indices—experienced a sharp downturn beginning mid-February 2020. This paper seeks to quantify the causal impact of the COVID-19 recession on the log returns of the S&P 500 using causal inference techniques. Our approach combines the Synthetic Control Method (SCM) with stochastic volatility modeling to account for the uncertainty in returns and smoothness over time.

Traditional comparative methods fall short in such macroeconomic shocks due to the lack of a clear untreated group. The synthetic control approach mitigates this limitation by constructing a counterfactual using a weighted combination of other markets. We begin by using global equity indices to build this counterfactual, but find the fit unsatisfactory. To enhance robustness, we include commodities, whose behavior differs significantly from equity markets and can serve as a diversified benchmark.

To further assess the impact and control for return volatility, we apply a Gibbs sampler to estimate stochastic volatility models separately for the actual and synthetic returns. This dual approach enables us to evaluate both level and volatility effects, especially in a focused post-treatment window around the event.

2 Background and Methodological Framework

Understanding the economic consequences of global shocks like COVID-19 is crucial not only for historical analysis but also for informing future policy responses and financial decision-making. Financial indices such as the S&P 500 encapsulate the expectations, fears, and behaviors of a broad spectrum of economic actors, and their reaction to crises can provide a barometer for economic health and investor sentiment.

The S&P 500, in particular, is often viewed as a proxy for the broader U.S. economy and serves as a benchmark for trillions of dollars in investment. Quantifying the causal effect of unexpected shocks on such an index is therefore a problem of considerable importance for economists, policymakers, and financial institutions alike.

Moreover, distinguishing between fundamental economic impacts and transient market behavior requires careful modeling. By applying a synthetic control approach and pairing it with stochastic volatility analysis,

we aim to tease out not just directional changes but also changes in market uncertainty. The methods used here illuminate both the trajectory and the instability of market responses, offering insights into how resilient or reactive financial systems are during global crises.

2.1 Synthetic Control Method (SCM)

SCM constructs a weighted average of control units to approximate the counterfactual outcome of a treated unit had the treatment not occurred (Abadie 2003, Abadie 2010). In this setting, the treated unit is the S&P 500 log return time series, and the treatment is the onset of COVID-19-induced recession effects starting February 13, 2020.

Let Y_{1t}^N be the potential outcome of the treated unit $i = 1$ in the absence of treatment, and Y_{1t}^I the observed outcome under intervention. The synthetic control estimator is:

$$\hat{Y}_{1t}^N = \sum_{j=2}^{J+1} w_j Y_{jt}, \tag{1}$$

where weights w_j are chosen to minimize the pre-treatment discrepancy between Y_{1t} and the weighted combination of Y_{jt} for $t < T_0$.

In the fully correlated series approach, we construct the donor pool using major global indices: $\hat{\texttt{D}}\texttt{JI}$, $\hat{\texttt{I}}\texttt{XIC}$, $\hat{\texttt{R}}\texttt{UT}$, $\hat{\texttt{F}}\texttt{TSE}$, $\hat{\texttt{N}}\texttt{225}$, and $\hat{\texttt{H}}\texttt{SI}$. The synthetic control derived from these sources fits the pre-treatment path of the S&P 500 relatively well, but exhibits limitations in capturing the volatility spike and subsequent stabilization during the COVID-19 shock. The post-treatment MSPE of approximately 5.70×10^{-6} and synthetic weights heavily concentrated on the $\hat{\texttt{I}}\texttt{XIC}$ index (weight: 0.645) indicate limited diversification. This approach results in a control that fails to absorb the idiosyncratic features of the actual returns during crisis periods, producing high variance in the post-COVID tracking plot.

To address these limitations, we extended the donor pool to include commodities, leading to a more stable and contextually informed synthetic control. The improved model reduces spurious volatility and tracks the actual returns more faithfully in the post-treatment period.

2.2 Average Treatment Effect on the Treated (ATET)

We define the ATET as the average difference between actual and synthetic S&P 500 returns post-treatment:

$$\text{ATET} = \frac{1}{T} \sum_{t=T_0}^{T_1} \left(Y_{1t}^I - \hat{Y}_{1t}^N \right),$$

where T_0 is the treatment start date and T_1 is the end of the observation window.

2.3 Stochastic Volatility Model via Gibbs Sampling

Stochastic volatility (SV) models are a class of time series models in which the variance of the error term evolves over time according to a latent stochastic process. This modeling framework, originally proposed by Taylor (1982), is particularly well-suited for financial return series, which typically exhibit volatility clustering—alternating periods of high and low variance.

Compared to ARCH-type models (Engle, 1982), SV models provide greater flexibility and realism by incorporating two distinct stochastic processes: one for the observed data and another for the latent volatility. This makes SV models especially appropriate for analyzing financial data, where volatility is not directly observed but must be inferred.

Model Specification

The discrete-time SV model we use is defined as follows defined in Kim (1998):

$$\begin{aligned} y_t &= \beta e^{h_t/2}\varepsilon_t, && \text{for } t = 1, \ldots, T, \\ h_{t+1} &= \mu + \phi(h_t - \mu) + \sigma_\eta \eta_t, \\ h_1 &\sim \mathcal{N}\left(\mu, \frac{\sigma_\eta^2}{1-\phi^2}\right), \end{aligned}$$

where:

- y_t is the mean-adjusted return of an asset at time t.
- $\varepsilon_t \sim \mathcal{N}(0,1)$ are i.i.d. shocks to the return process.
- h_t is the latent log-volatility at time t.
- μ is the unconditional mean of the log-volatility process.
- ϕ is the persistence parameter, with stationarity requiring $|\phi| < 1$.
- $\eta_t \sim \mathcal{N}(0,1)$ are i.i.d. innovations to the volatility process.
- σ_η^2 controls the variance of the volatility process.
- β is typically set to 1 for identification (we follow Kim, 1998).

Bayesian Estimation and Posterior Sampling

To estimate the SV model, we adopt a Bayesian approach, which involves drawing samples from the joint posterior distribution:

$$p(\mu, \phi, \sigma_\eta^2, h_{1:T} \mid y_{1:T}).$$

This posterior is highly complex and high-dimensional, making direct sampling infeasible. Instead, we apply a Gibbs sampler—an MCMC technique that mitigates the curse of dimensionality by breaking the joint posterior into its full set of conditional distributions, from which efficient sampling is possible.

Following the implementation by Meng (2009), we set priors for the parameters μ, ϕ, and σ_η^2, and iteratively draw from their full conditional distributions. This allows us to construct posterior distributions for each latent volatility path $\{h_t\}$.

Application and Interpretation

By fitting the SV model to both the actual and synthetic return series, we can compare not just the average behavior, but the full posterior distribution of volatility over time. This facilitates causal inference in settings where volatility itself—rather than return levels—may be impacted by events such as financial crises.

In particular, we analyze the interval from February 1 to May 30, 2020, which captures the market's short-run response to the COVID-19 pandemic. The SV model's autoregressive structure smooths volatility paths while still allowing identification of meaningful deviations, thus providing a nuanced view of market instability.

3 Methodology

3.1 Synthetic Control Estimation: Implementation and Evaluation

The Synthetic Control Method (SCM) is a data-driven technique for estimating the counterfactual behavior of a treated unit by constructing a synthetic control—a weighted average of multiple control units—that closely matches the treated unit's behavior in the pre-treatment period. In our context, the treated unit is the daily log returns of the S&P 500 index, and the intervention is the onset of the COVID-19 shock starting February 13, 2020.

Step 1: Data Preparation

Daily closing prices were collected for the S&P 500 and a candidate donor pool using Yahoo Finance via the `quantmod` package in R. These prices were converted into log returns to stabilize variance and capture relative changes. The dataset spanned from January 1, 2018, to March 15, 2022. We reshaped the merged time series data into a panel format compatible with the `Synth` package.

Initially, our donor pool consisted of six major global equity indices: D̂JI, ÎXIC, R̂UT, F̂TSE, N̂225, and ĤSI. These were selected for their scale, liquidity, and representativeness of international equity markets.

Step 2: SCM Model Setup

Using the `dataprep()` function, we created matrices:

- X_1: predictor values for the treated unit (S&P 500)
- X_0: predictor values for the control units
- Z_1: outcome values for the treated unit (S&P 500 returns)
- Z_0: outcome values for the control units

We treated the return series itself as the predictor and outcome, given the short daily frequency and consistent nature of the time series. The pre-treatment period was used both to select optimal weights and to evaluate the synthetic match.

Step 3: Weight Optimization

The `synth()` function optimizes a weighted combination of control units such that the pre-treatment trajectory of the synthetic control closely approximates the actual S&P 500. The optimization minimizes the following loss function:

$$\min_{w}(X_1 - X_0 w)' V (X_1 - X_0 w) \tag{2}$$

subject to $w_j \geq 0$ and $\sum w_j = 1$, where V is a matrix that can be tuned for predictor importance. We used default settings where V is estimated within the function.

Rationale for Dual Donor Pools

Our initial donor pool, composed solely of equity indices, resulted in high correlation with the treated unit due to similar global market behavior. For instance, both the Dow Jones and NASDAQ are U.S.-based and thus structurally similar to the S&P 500. This collinearity can inflate the precision of the pre-treatment fit while undermining the distinctiveness of the counterfactual.

To reduce this redundancy and introduce orthogonal behavior, we expanded the donor pool to include commodity futures (e.g., gold, oil, silver, copper, corn). These markets react differently to macroeconomic forces, geopolitical events, and supply-side shocks, providing a richer and more behaviorally diverse basis for constructing the synthetic control. The idea is that these are less cointegrated with the main series and as a result by mixing the commodities with the other market indicators, we have a stronger donor pool to account for the structural change.

Both donor sets were processed using identical SCM procedures. The only change was the content of the control matrix X_0 and the resulting optimal weight distribution. The broader control pool allows SCM to construct a counterfactual that is not overly dependent on highly correlated financial instruments, improving interpretability and reducing post-treatment distortion.

To analyze the results of the synthetic control, we utilized the ATET formula defined above and computed the difference in the two returns' time series.

3.2 Stochastic Volatility Estimation via Gibbs Sampling

To estimate the time-varying volatility of financial returns, we implement a stochastic volatility (SV) model using a custom Gibbs sampling algorithm. This model is particularly appropriate for financial data exhibiting volatility clustering and allows us to assess how volatility evolves under treatment (i.e., post-COVID) conditions.

Algorithmic Implementation

We follow the approach of Kim (1998) and Meng (2009) and implement the algorithm as follows:

- Initialize $(h^{(0)}, \sigma_\eta^{2(0)}, \phi^{(0)}, \mu^{(0)})$
- **Start Cycle One:**
  - Sample $h_1^{(1)} \sim \mathcal{N}\left(\mu, \frac{\sigma_\eta^2}{1-\phi^2}\right)$
  - Sample $h_t^{(1)}$ for $t = 2, \ldots, T$ conditional on surrounding h values
  - Sample $\sigma_\eta^{2(1)} \sim f(\sigma_\eta^2 \mid y, h^{(1)}, \phi^{(0)}, \mu^{(0)})$
  - Sample $\phi^{(1)} \sim f(\phi \mid y, h^{(1)}, \sigma_\eta^{2(1)}, \mu^{(0)})$
  - Sample $\mu^{(1)} \sim f(\mu \mid y, h^{(1)}, \sigma_\eta^{2(1)}, \phi^{(1)})$
- **Repeat** this sequence for M cycles

The update for h_t is performed via accept-reject sampling with proposals drawn from:

$$\mathcal{N}(\mu_t, \nu^2), \quad \text{where } \nu^2 = \frac{\sigma_\eta^2}{1+\phi^2},$$

and

$$\mu_t = h_t^\star + \frac{\nu^2}{2}\left[y_t^2 \exp(-h_t^\star) - 1\right], \quad \text{with } h_t^\star = \mu + \frac{\phi(h_{t-1} - \mu + h_{t+1} - \mu)}{1+\phi^2}.$$

The acceptance ratio is computed via:

$$\log f^*(y_t, h_t, \theta) = -\frac{1}{2}h_t - \frac{y_t^2}{2}\exp(-h_t),$$
$$\log g^*(y_t, h_t, \theta) = -\frac{1}{2}h_t - \frac{y_t^2}{2}\left[\exp(-h_t^\star)(1 + h_t^\star) - h_t \exp(-h_t^\star)\right].$$

This procedure ensures valid samples from the posterior of each latent volatility state h_t under the correct full conditional distribution.

Why Gibbs Sampling?

The choice of Gibbs sampling is deliberate: it is a powerful and flexible algorithm for approximating complex posterior distributions, particularly in models with many interdependent parameters. The joint posterior distribution

$$p(\mu, \phi, \sigma_\eta^2, h_{1:T} \mid y_{1:T})$$

is analytically intractable due to its high dimensionality and nonlinear structure. Gibbs sampling circumvents this by iteratively sampling from full conditional distributions—each of which is easier to sample from than the joint.

This makes Gibbs sampling an ideal candidate for exploring large parameter spaces, where closed-form solutions are unavailable and numerical optimization is impractical. Its modular nature also enables targeted control and diagnostics at each step, which is critical when working with latent structures such as volatility.

Why Custom Implementation?

Although several R packages (e.g., `stochvol`) provide stochastic volatility samplers, these packages abstract away essential components, limiting customizability. For our purpose—comparing volatility dynamics between synthetic and actual returns in a highly specific temporal window—a custom implementation was preferred. It allowed for:

- Full transparency and control over the sampling logic and priors
- Adjustment of acceptance criteria for h_t updates

- Monitoring convergence through manual diagnostics and burn-in plots
- Consistent structure across synthetic and actual model implementations

This level of control was essential to ensure comparability and to extract meaningful insights from post-COVID market behavior.

Dual Implementation

This procedure is applied separately to both the actual and synthetic S&P 500 return series. Each run of the Gibbs sampler involves 15,000 iterations, with the first 5,000 discarded as burn-in. This allows us to generate posterior distributions over volatility dynamics for each regime and quantify how volatility behavior differs due to the COVID-19 shock.

The algorithm's implementation provides smoothed latent volatility paths and posterior summaries of uncertainty, which we leverage in later sections to compare the resilience and instability between the treated and counterfactual financial time series.

4 Results

4.1 Synthetic Control Method: Market Indicator Donors

Our initial implementation of the Synthetic Control Method used six major market indices as donor units: D̂JI, ÎXIC, R̂UT, F̂TSE, N̂225, and ĤSI. The dataprep object generated the X_1, X_0, Z_1, and Z_0 matrices based on these returns. These inputs allowed the `synth()` function to compute an optimal synthetic control, minimizing the pre-treatment squared loss between the actual and synthetic series.

The optimization results are as follows:

```
****************
 optimization over w weights: computing synthetic control unit
****************
****************
****************
MSPE (LOSS V): 5.696694e-06
solution.v:
1
solution.w:
0.1038719 0.6445169 0.08243833 0.06595751 0.05530426 0.04791119
```

The synthetic control is heavily concentrated on the ÎXIC index, receiving a weight of approximately 0.645. This suggests that the S&P 500's pre-COVID return behavior is most closely mimicked by the NASDAQ, which is unsurprising given their overlap in market exposure. However, this collinearity weakens the post-treatment inference. Because both indices react similarly to global economic shocks, the synthetic control fails to differentiate itself significantly from the treated unit after the onset of COVID-19.

Figure 1 shows a strikingly close match between the actual and synthetic return paths in both the pre- and post-treatment periods. This is a poor control: the synthetic is unable to diverge from the treated path when a real economic shock hits, suggesting it has simply replicated the treated series' own behavior. In causal inference terms, this undermines our counterfactual credibility.

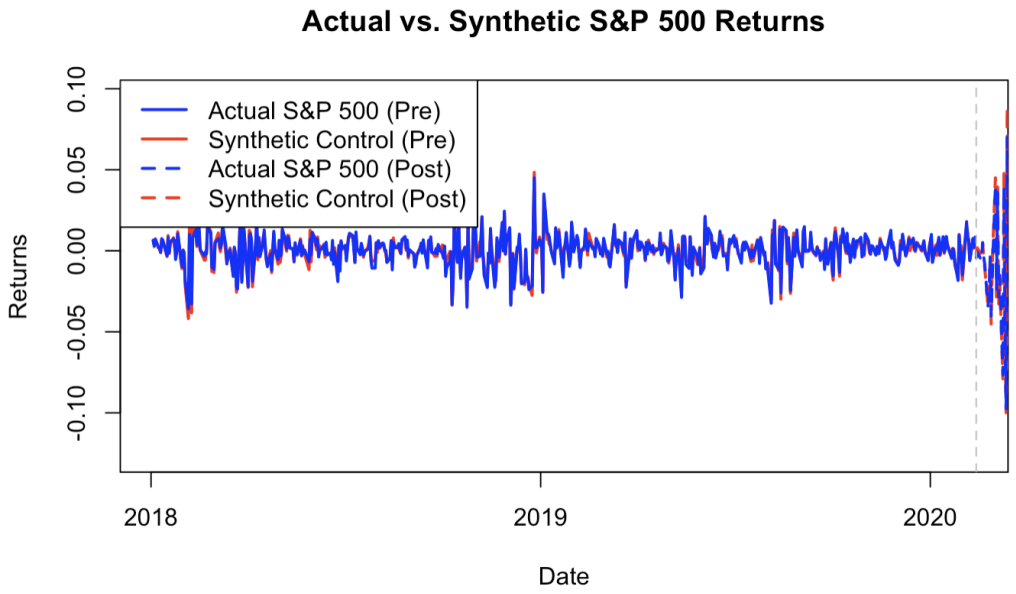

Figure 1: Actual vs. Synthetic S&P 500 Returns Using Market Indicators (Full Period)

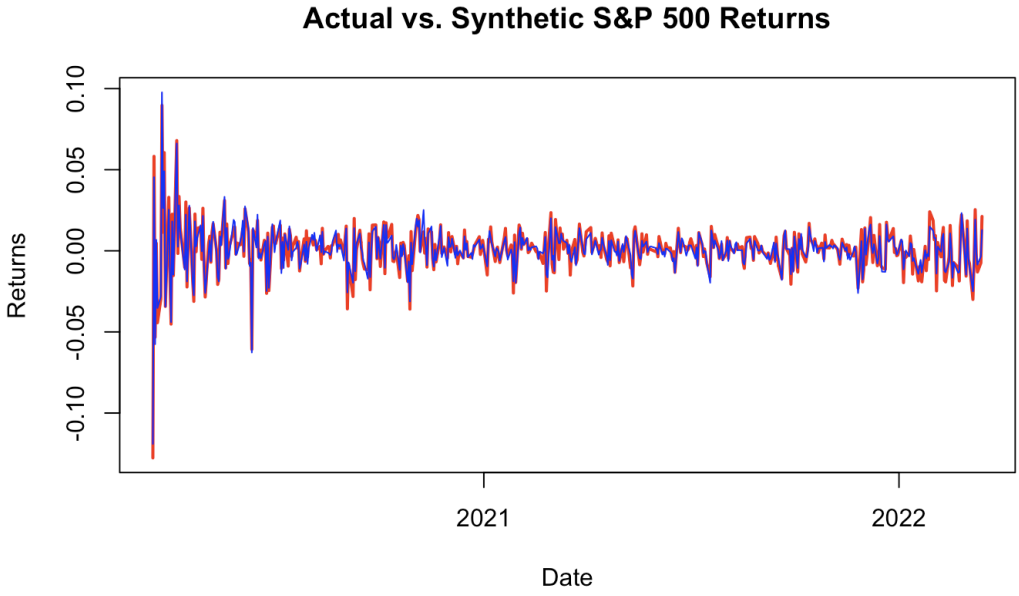

Figure 2: Actual vs. Synthetic S&P 500 Returns Using Market Indicators (Post-COVID Only)

These results confirm that while the synthetic control accurately tracks the actual S&P 500 during stable periods, it fails to capture a structural break such as COVID-19's impact. This highlights a core limitation of using highly correlated equity indices as the sole basis for synthetic control construction.

4.2 Synthetic Control Method: Mixed Commodity Donors

To address the limitations of the initial model, we expanded the donor pool to include a diverse set of commodity futures in addition to equity indices. The revised donor pool included: CL=F, GC=F, SI=F, HG=F, BZ=F, NG=F, ZC=F, ZS=F, D̂JI, ÎXIC, R̂UT, F̂TSE, N̂225, and ĤSI. These additions brought economic behaviors into the model that were less synchronized with the S&P 500, such as commodity price sensitivity to supply chain disruptions and geopolitical shifts.

The resulting optimization yielded the following output:

```
****************
 optimization over w weights: computing synthetic control unit
****************
****************
****************
MSPE (LOSS V): 6.577816e-06
solution.v:
1
solution.w:
0.01764264 0.03779525 0.02631587 0.01564253 0.01722679 0.008796385
0.0300996 0.0217193 0.0375783 0.6913081 0.03045981 0.02499004
0.02144353 0.01898187
```

Most notably, the largest individual weight (˜69%) is now placed on ÎXIC, but other weights are distributed across the remaining 13 commodities and indices. This dispersion reduces the model's reliance on any single correlated equity market, introducing heterogeneity into the synthetic control's response dynamics. This makes it a stronger approach to identifying a control.

Figures 3 and 4 demonstrate that the mixed model synthetic control deviates meaningfully from the actual S&P 500 in the post-COVID period. This divergence suggests that the synthetic control now captures a plausible counterfactual path—how the S&P 500 might have behaved had COVID-19 not occurred.

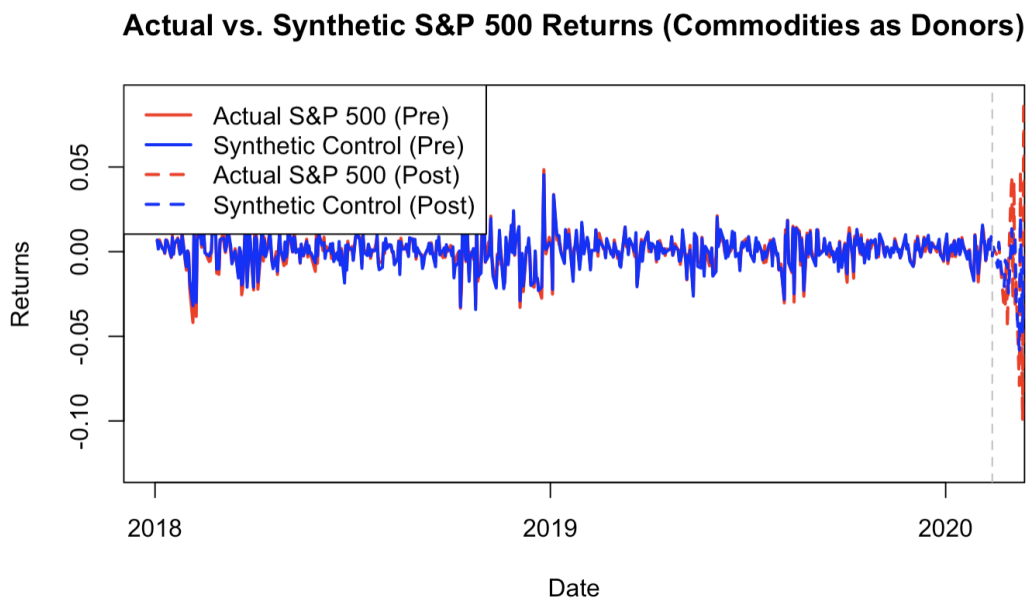

Figure 3: Actual vs. Synthetic S&P 500 Returns (Commodities as Donors, Full Period)

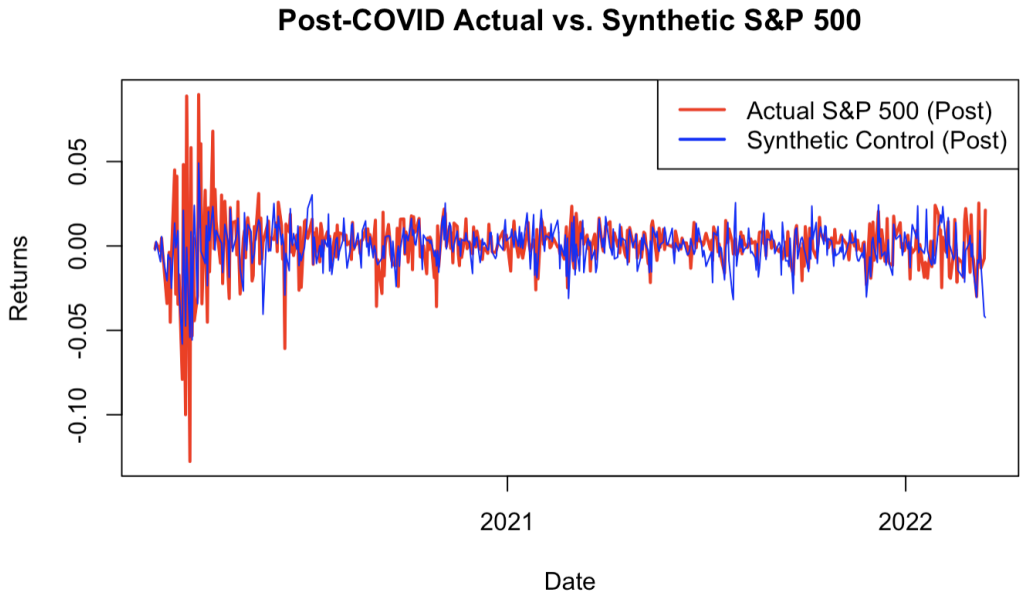

Figure 4: Post-COVID Actual vs. Synthetic S&P 500 Returns (Commodities as Donors)

To evaluate the causal effect, we compute the Average Treatment Effect on the Treated (ATET) by taking the mean return difference between actual and synthetic in the post-treatment window:

```
[1] "Average Treatment Effect (Post-COVID): 0.000647"
```

The small but persistent positive difference suggests that the real S&P 500 recovered slightly faster than the counterfactual path predicted by the synthetic control. This could be attributed to large-scale government stimulus and liquidity interventions in financial markets, which may not be fully priced into the donor asset classes.

The return differences are visualized in Figure 5, where we observe a spike in deviation during early COVID-19 weeks and gradual convergence thereafter.

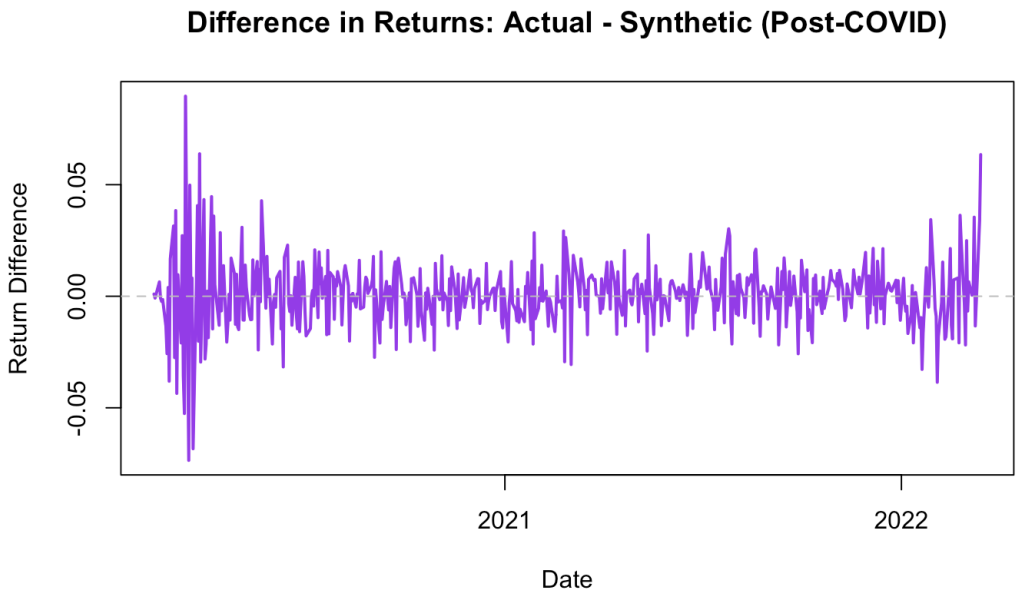

Figure 5: Difference in Returns: Actual - Synthetic (Post-COVID)

Taken together, these results affirm the need for diverse donor pools in constructing synthetic controls, especially in the presence of global shocks. The commodity-enriched control provides a more credible and dynamic counterfactual, revealing subtle but meaningful differences in S&P 500 behavior attributable to the pandemic.

4.3 Stochastic Volatility Modeling: Actual vs. Synthetic Returns

After applying the Synthetic Control Method, we turned to stochastic volatility modeling to assess how market uncertainty evolved following the onset of COVID-19. This modeling approach was applied separately to both the actual and synthetic return series.

We first estimated volatility using the full return series (January 2018–March 2022) for both actual and synthetic paths. Then, to detect more granular divergence, we fit the model again using a reduced 61-day window beginning February 3, 2020. In both cases, the stochastic volatility model was estimated using our custom Gibbs sampling algorithm described in the above sections.

4.3.1 Full-Length Volatility Estimation

The full-sample volatility plots, shown in Figures 6 and 7, reveal a sharp volatility spike beginning in February 2020, peaking shortly after the pandemic-triggered crash. This is consistent with market narratives and news coverage from the time.

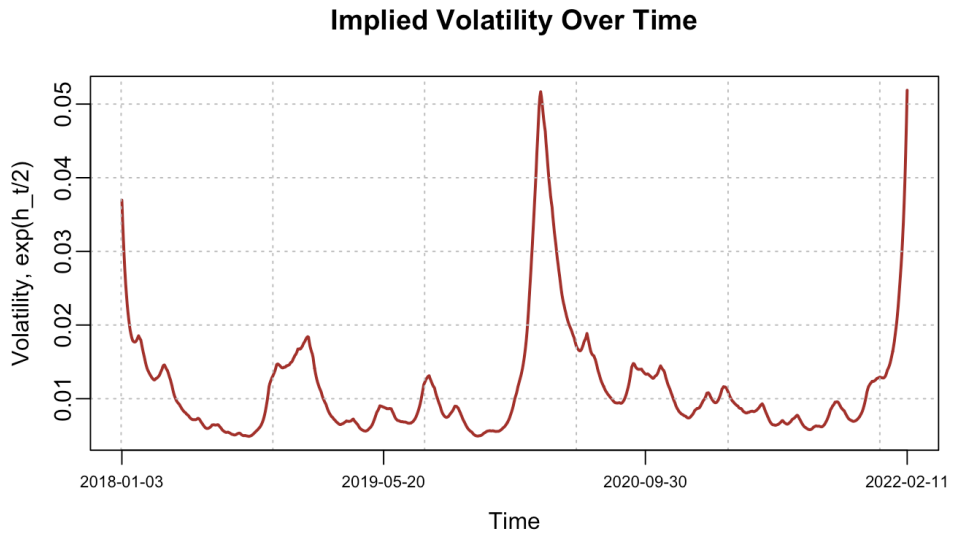

Figure 6: Actual Return Series: Implied Volatility Over Time (Full Sample)

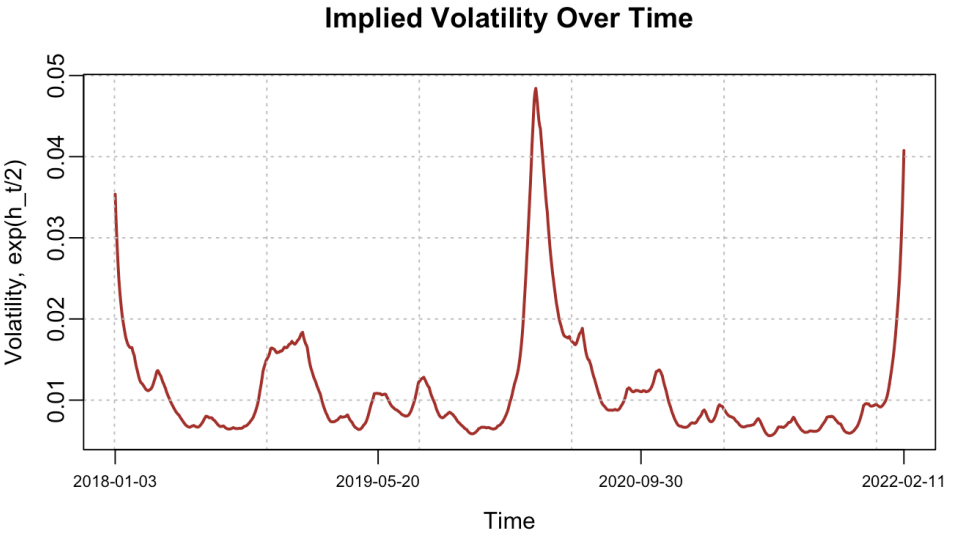

Figure 7: Synthetic Return Series: Implied Volatility Over Time (Full Sample)

The full-sample posterior summaries support these visual impressions:

- **Actual Returns (Full)**: $\sigma^2 \approx 4.82 \times 10^{-5}$, $\phi \approx 0.997$, $\mu \approx -6.60$, $\beta \approx 0.036$
- **Synthetic Returns (Full)**: $\sigma^2 \approx 4.82 \times 10^{-5}$, $\phi \approx 0.997$, $\mu \approx -6.68$, $\beta \approx 0.0358$

These estimates are strikingly similar across both models, suggesting that the volatility structure of the synthetic control closely mirrors that of the actual S&P 500—at least when examined over a long horizon.

The trace plots and ACF diagnostics in Figures 8 and 9 confirm adequate convergence and mixing. Meaning that the sampler properly explored the parameter space.

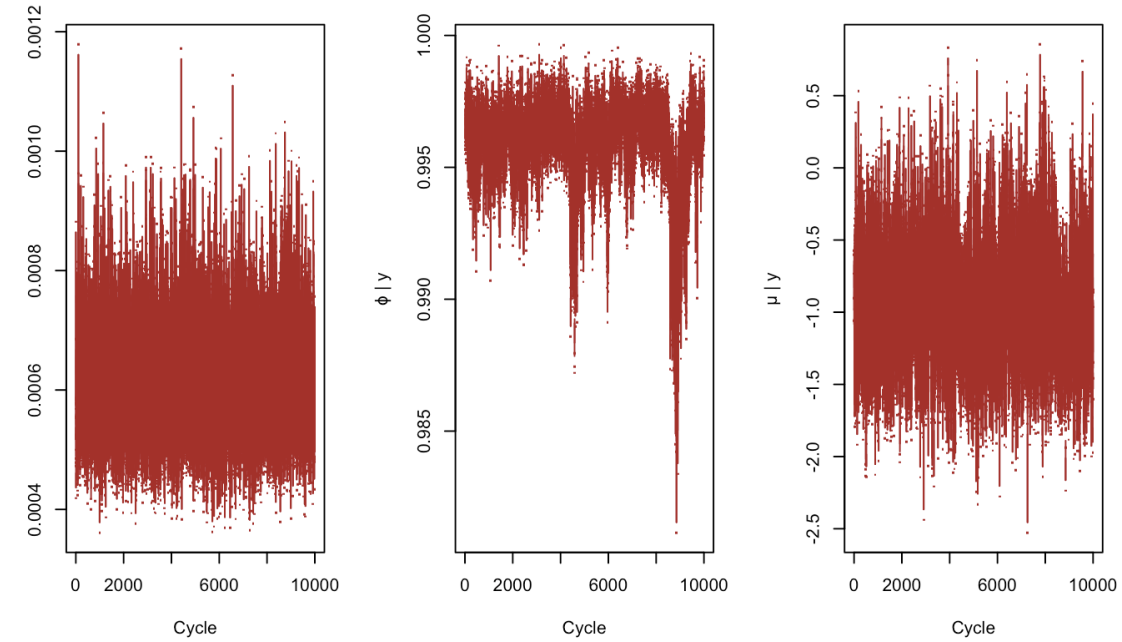

Figure 8: Actual Return Series: Trace Plots for Full Sample with Burn-in

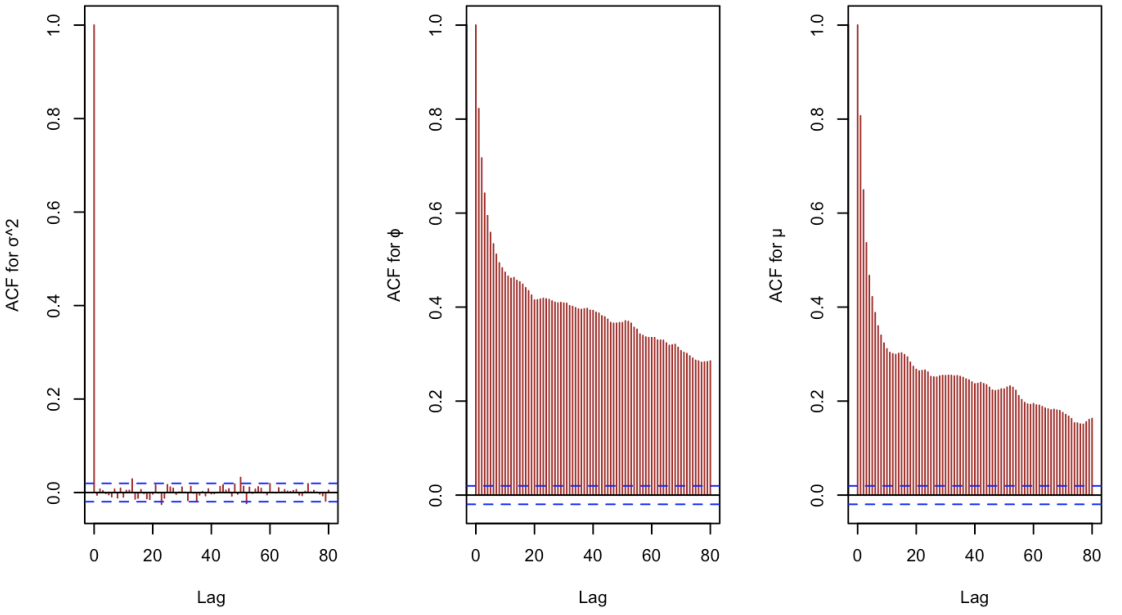

Figure 9: Actual Return Series: ACF for Full Sample

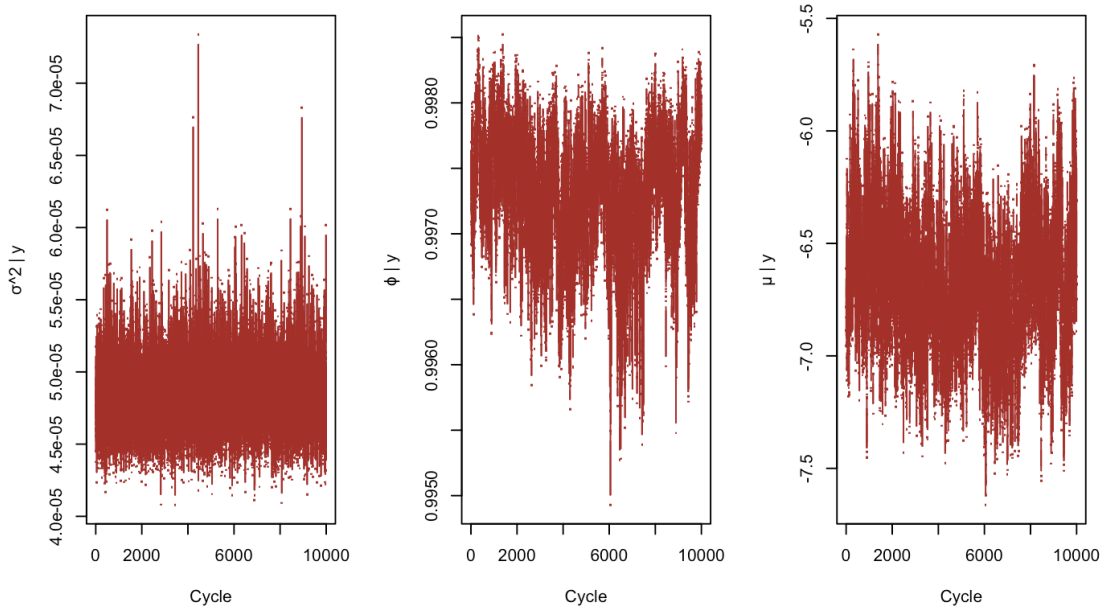

Figure 10: Synthetic Return Series: Trace Plots for Full Sample with Burn-in

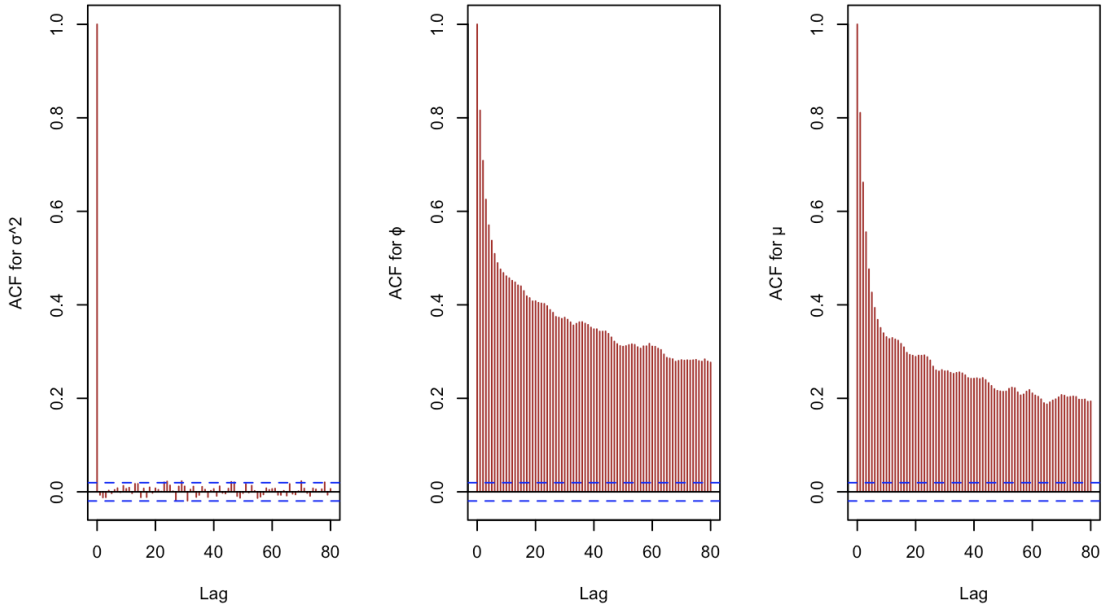

Figure 11: Synthetic Return Series: ACF for Full Sample

4.3.2 Reduced-Window Volatility Estimation (Feb–Apr 2020)

To uncover localized differences, we ran the SV model again using only 61 days of data starting from early February 2020. Figures 12 and 13 show the implied volatility paths.

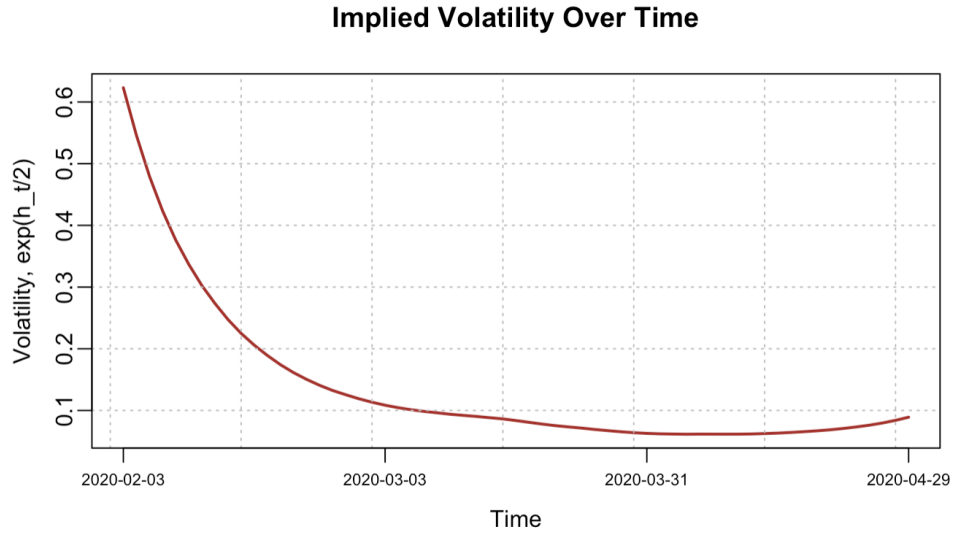

Figure 12: Actual Return Series: Implied Volatility Over Time (Feb–Apr 2020)

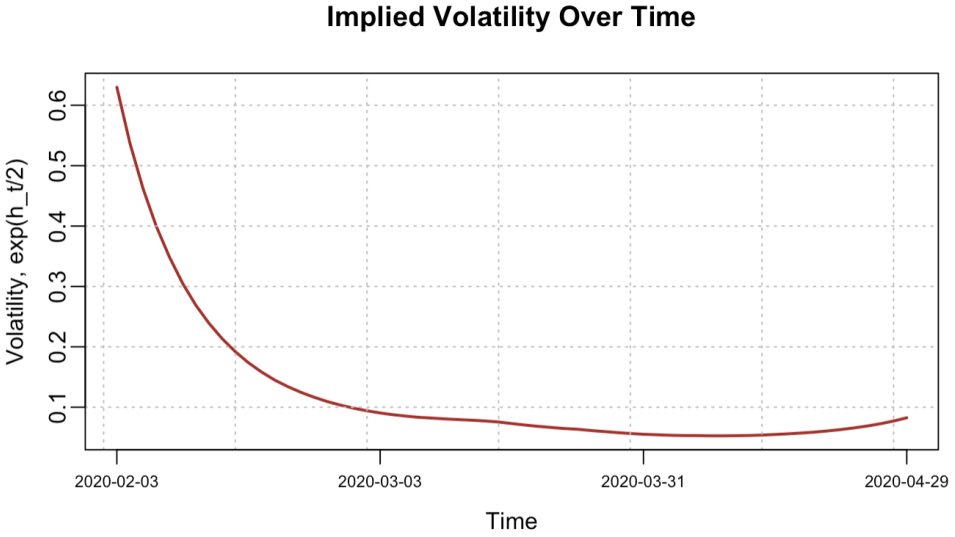

Figure 13: Synthetic Return Series: Implied Volatility Over Time (Feb–Apr 2020)

We do observe modest divergence between the two series during this interval. Volatility is higher in the actual series during the first few weeks of the crash. However, both curves quickly converge toward a common lower baseline. This is likely due to:

- The smoothing properties of the stochastic volatility model, which interpolates between points through an AR(1) latent log-volatility process
- Government intervention and market stabilization after the initial crash, which affected both series similarly

- The limitations of a 61-day window in capturing regime switches under strong autoregressive persistence ($\phi \approx 0.996$)

Posterior summaries for the reduced model window are as follows:

- **Actual Returns (Short)**: $\sigma^2 \approx 0.000608$, $\phi \approx 0.9960$, $\mu \approx -0.949$, $\beta \approx 0.637$
- **Synthetic Returns (Short)**: $\sigma^2 \approx 0.000605$, $\phi \approx 0.9964$, $\mu \approx -0.925$, $\beta \approx 0.644$

Again, the estimates are close—but no longer identical. This supports the idea that short-term volatility behavior does deviate slightly between actual and counterfactual worlds, though not dramatically.

Figures 14–17 provide diagnostic support for these estimates.

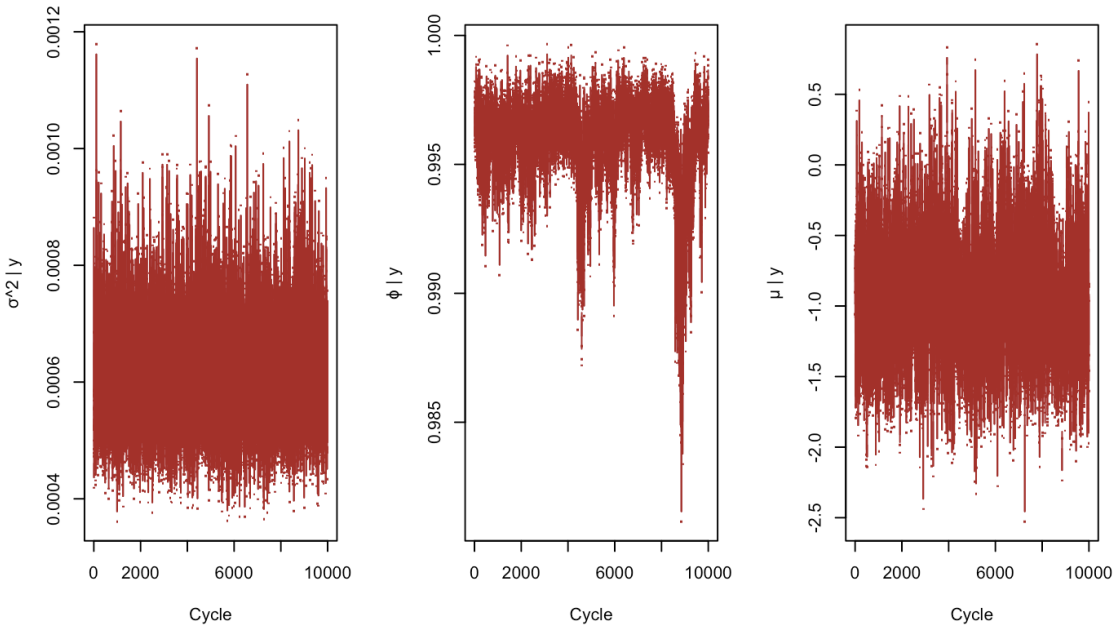

Figure 14: Actual Return Series: Trace Plots with Burn-in (Short Window)

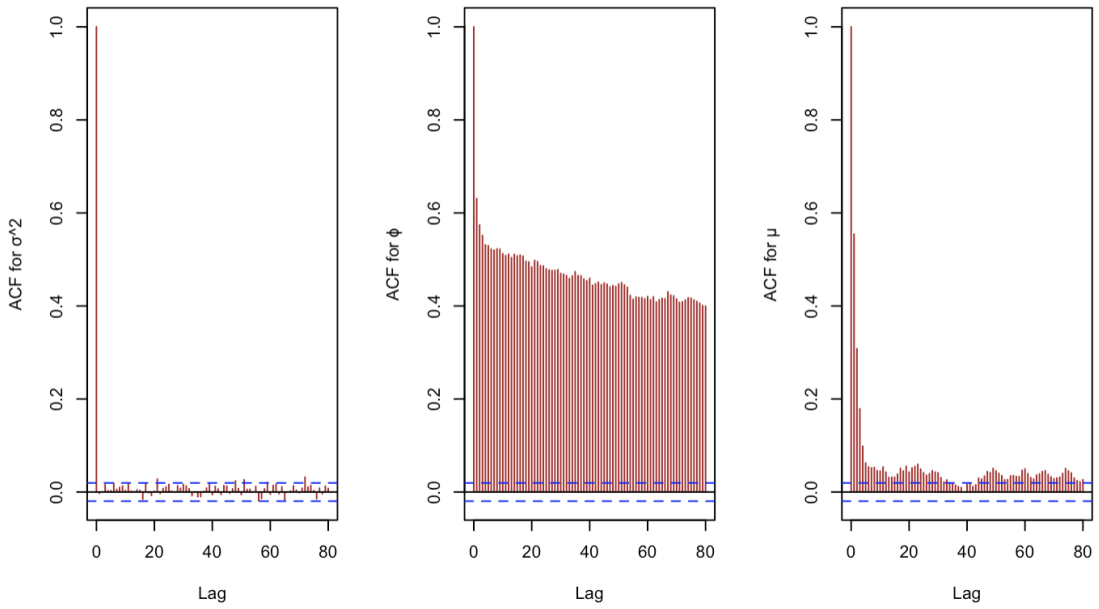

Figure 15: Actual Return Series: ACF Plots (Short Window)

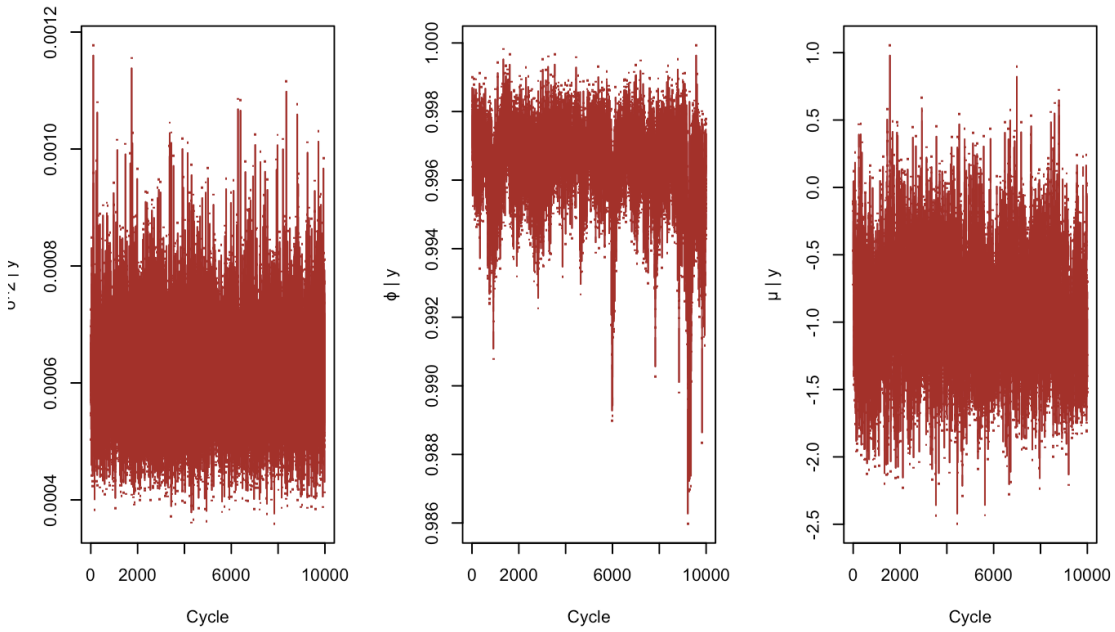

Figure 16: Synthetic Return Series: Trace Plots with Burn-in (Short Window)

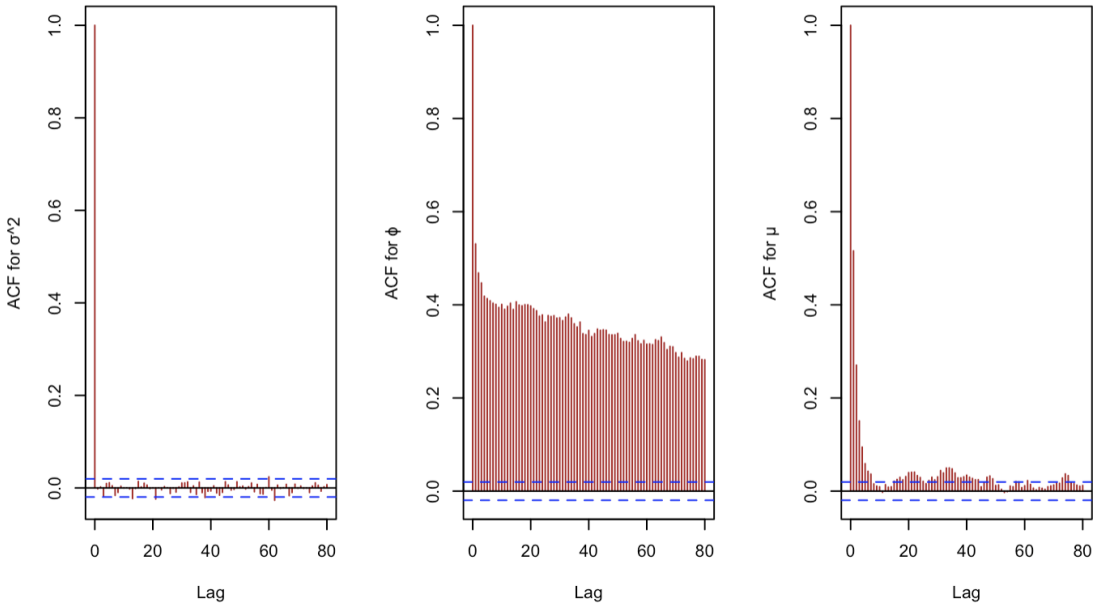

Figure 17: Synthetic Return Series: ACF Plots (Short Window)

4.3.3 Direct Comparison of Posterior Volatility

To further quantify the similarity in volatility dynamics, we directly compared the posterior draws from the actual and synthetic volatility processes in both the full and short windows using scatterplots. These are shown in Figures 18 and 19.

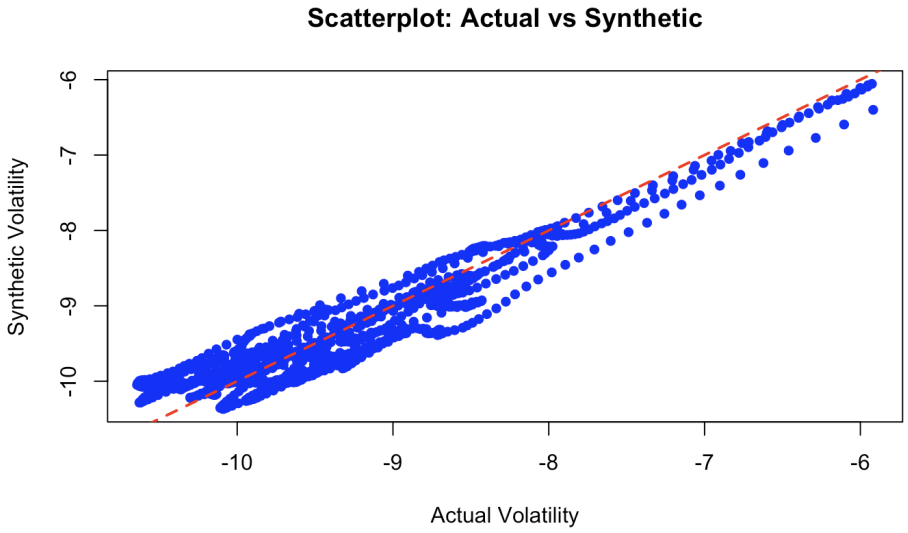

Figure 18: Scatterplot: Actual vs Synthetic Volatility (Full Sample)

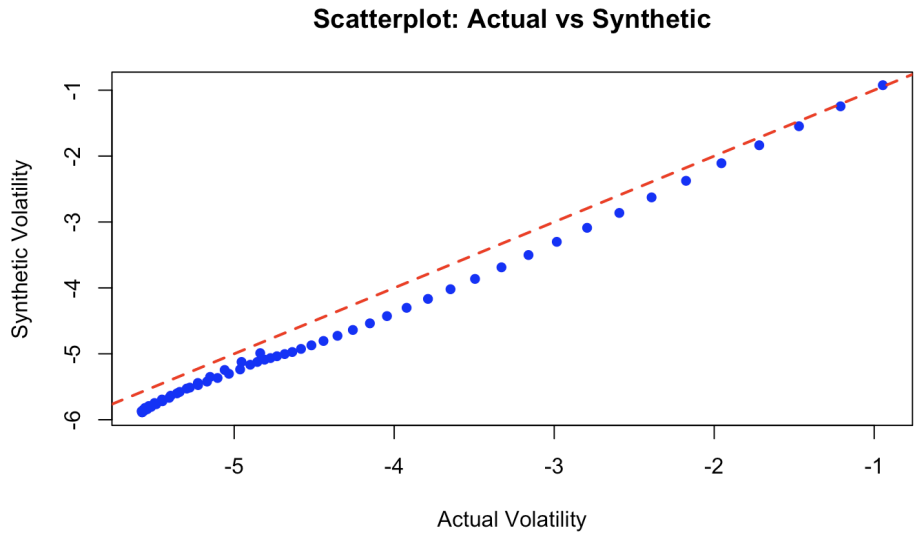

Figure 19: Scatterplot: Actual vs Synthetic Volatility (Short Sample)

In the short/subset time period comparison, the posterior volatility estimates align well with the $y = x$ line (y=x implies that the values are the same. This suggests near-identical behavior over the entire period. In the short window, we observe slight deviations from the diagonal, but the estimates remain tightly clustered.

We see in the histograms of the differences that while the values are generally small, they are not zero. In the short window, the differences are skewed and strictly positive, suggesting higher short-term volatility in the actual series. In contrast, the full-sample differences are more symmetrically distributed around zero, supporting the conclusion that the Gibbs sampler smooths out local shocks over longer periods.

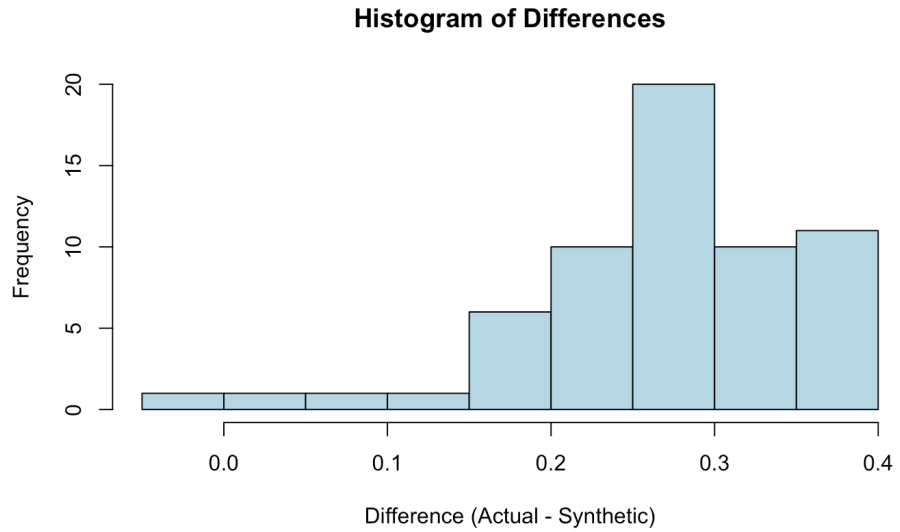

Figure 20: Histogram: Actual - Synthetic (Short Sample)

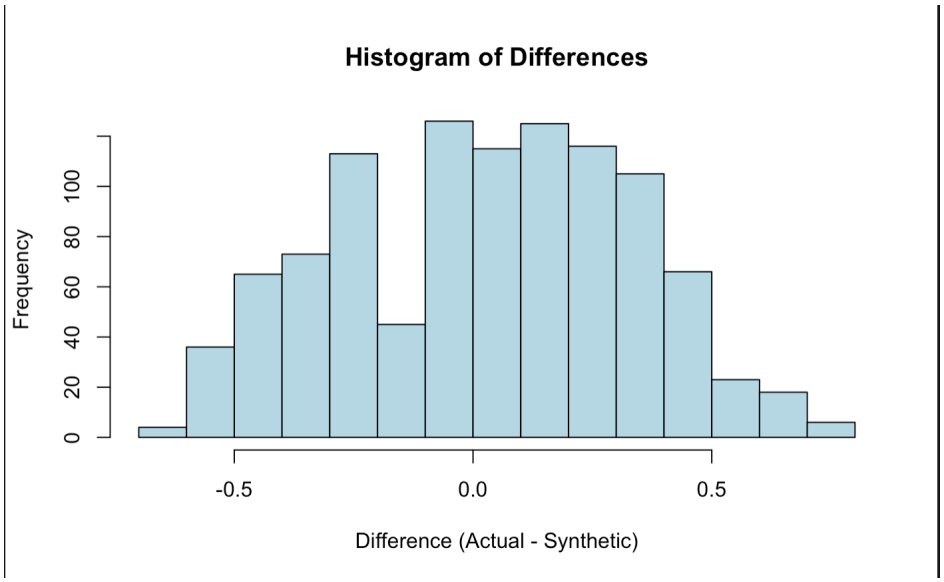

Figure 21: Histogram: Actual - Synthetic (Full Sample)

These scatterplots reinforce the conclusion that if two return series are closely matched and centered around zero—as log returns typically are—then the implied volatility estimates from a Gibbs sampler SV model will tend to be very similar. This is due not only to the similarity of the underlying data but also to the inherent smoothing behavior of the model.

4.3.4 Discussion

Overall, we find strong consistency in volatility dynamics across actual and synthetic paths. The near-identical posterior estimates in the full model suggest that both time series experienced similar levels of underlying uncertainty over the entire horizon. The short-term model, while revealing subtle differences, still shows tight alignment in volatility behavior.

The direct scatterplot comparisons confirm this further: when return series are highly similar and centered (as is typical with log returns), the Gibbs sampler's smoothing characteristics lead to minimal divergence in volatility estimates. This occurs even when synthetic data is generated under different donor pools, as long as return-level similarity remains high.

This raises an important interpretation: the synthetic control may effectively mimic the risk dynamics of the S&P 500, even in crisis periods. However, the autoregressive structure of the SV model (with $\phi \approx 0.996$) dampens short-lived deviations and limits our ability to detect transitory volatility shocks.

Future work could explore modifications such as:

- Introducing jump processes or regime-switching volatility
- Segmenting time into multiple windows to capture local effects
- Using alternative priors or semi-parametric volatility structures

These refinements could enhance our ability to detect and attribute fine-grained differences in financial uncertainty post-intervention.

5 Conclusion

This study applied a dual-framework approach to evaluate the impact of the COVID-19 recession on the S&P 500, combining the Synthetic Control Method (SCM) with stochastic volatility (SV) modeling via Gibbs sampling. Our results show that while SCM with market-only donors produced a synthetic control

closely mirroring the actual S&P 500 pre-COVID, it failed to provide a meaningful counterfactual in the post-treatment period due to excessive correlation. By incorporating commodity futures into the donor pool, we introduced behavioral heterogeneity that enhanced the synthetic control's post-COVID divergence and interpretability.

Using the improved control, we estimated the Average Treatment Effect on the Treated (ATET) and found a modest but persistent deviation in post-treatment returns, suggesting a real effect of the COVID-19 shock. However, this level difference alone may not capture the full story—hence, we incorporated a custom Gibbs sampler to model latent volatility for both series. The SV results revealed near-identical volatility trajectories over the full period, and only slight divergence during a short COVID-critical window. These findings indicate that while the synthetic control succeeded in tracking volatility risk overall, short-term instability was slightly higher in the actual series—potentially reflecting the real market's greater sensitivity to uncertainty during crisis onset.

Together, these methods provided a robust causal framework, combining level-based and volatility-based inference to assess treatment effects from macroeconomic shocks. The Gibbs sampler proved particularly well-suited for exploring high-dimensional parameter spaces, offering smooth and interpretable volatility paths.

6 Future Work

While this paper provides a rigorous framework for causal inference using SCM and stochastic volatility modeling, several avenues for further research remain open:

- **Refining the Synthetic Control:** Future work could explore dynamic synthetic controls or machine learning–guided weighting schemes to better capture structural breaks. Introducing time-varying weights or local SCM estimators could allow the counterfactual to better respond to shocks.
- **Expanding the Donor Pool:** Although adding commodities improved model robustness, the donor set could be further enhanced with alternative asset classes (e.g., bond indices, real estate, or sectoral ETFs) that respond differently to global events.
- **Volatility Model Extensions:** The current SV model assumes continuous paths with smooth AR(1) dynamics. Extensions incorporating jump components, stochastic volatility with leverage, or regime-switching models (e.g., Markov switching SV) could better capture abrupt shifts in uncertainty during crisis periods.
- **Time-Localized Inference:** Segmenting the post-treatment period into multiple windows would allow detection of localized effects, especially given that volatility responses to macroeconomic shocks often evolve over time. Rolling estimation or state-space filters could also be employed.
- **Posterior Divergence Measures:** Additional comparison metrics—such as Kullback–Leibler divergence or Wasserstein distances between posterior volatility distributions—may offer finer-grained insights into where and how synthetic and actual paths differ.

Taken together, these improvements would enhance the capacity of synthetic control frameworks to serve as credible counterfactuals not just in return space, but in volatility and risk dynamics—an essential feature for financial and economic policy analysis under uncertainty.

References

Abadie, A., & Gardeazabal, J. (2003). The Economic Costs of Conflict: A Case Study of the Basque Country. *American Economic Review*, 93(1), 113–132. https://www.aeaweb.org/articles?id=10.1257/000282803321455188

Abadie, A., Diamond, A., & Hainmueller, J. (2010). Synthetic Control Methods for Comparative Case Studies: Estimating the Effect of California's Tobacco Control Program. *Journal of the American Statistical Association*, 105(490), 493–505. https://doi.org/10.1198/jasa.2009.ap08746

Ben-Michael, E., Feller, A., & Rothstein, J. (2021). The Augmented Synthetic Control Method. *Journal of the American Statistical Association*, 116(536), 1789–1803. https://doi.org/10.1080/01621459.2021.1929245

Meng, Y. (2009). Bayesian Analysis of a Stochastic Volatility Model. *U.U.D.M. Project Report 2009.1.*

Taylor, S. J. (1982). Financial returns modelled by the product of two stochastic processes – a study of daily sugar prices 1961–75. In O. D. Anderson (Ed.), *Time Series Analysis: Theory and Practice* (Vol. 1, pp. 203–226). North-Holland.

Puig, M. (n.d.). *An Introduction to Stochastic Volatility Models.* Retrieved from https://diposit.ub.edu/dspace/bitstream/2445/122290/2/memoria.pdf

Wee, B. (2024). Comparing MCMC Algorithms in Stochastic Volatility Models using Simulation Based Calibration. *arXiv:2402.12384* [stat.AP].

Kastner, G. (2016). *stochvol: Efficient Bayesian Inference for Stochastic Volatility Models.* R package version 1.4. https://cran.r-project.org/web/packages/stochvol/index.html

Engle, R. F. (1982). Autoregressive Conditional Heteroscedasticity with Estimates of the Variance of United Kingdom Inflation. *Econometrica*, 50(4), 987–1007. https://doi.org/10.2307/1912773

Kim, S., Shephard, N., & Chib, S. (1998). Stochastic Volatility: Likelihood Inference and Comparison with ARCH Models. *The Review of Economic Studies*, 65(3), 361–393.

Gelfand, A. E., & Smith, A. F. M. (1990). Sampling-Based Approaches to Calculating Marginal Densities. *Journal of the American Statistical Association*, 85(410), 398–409.

Athey, S., & Imbens, G. (2017). The State of Applied Econometrics: Causality and Policy Evaluation. *Journal of Economic Perspectives*, 31(2), 3–32. https://doi.org/10.1257/jep.31.2.3

Zhang, D., Hu, M., & Ji, Q. (2020). Financial Markets under the Global Pandemic of COVID-19. *International Review of Financial Analysis*, 71, 101526. https://doi.org/10.1016/j.irfa.2020.101526

Synth Package: Source code for `synth()` function. Retrieved from https://github.com/cran/Synth/blob/master/R/synth.R

Note: To access all code used in this project, visit the GitHub repository: https://github.com/ReetomGangopadhyay/scm_sv_estimation